



Published in final edited form as:

ACS Biomater Sci Eng. 2015 ; 1(12): 1300–1305. doi:10.1021/acsbomaterials.5b00356.

Nanofibrous Snake Venom Hemostat

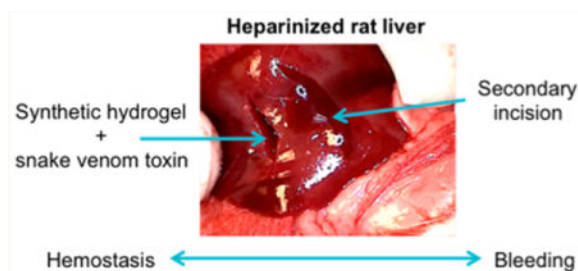
Vivek A. Kumar, Navindee C. Wickremasinghe, Siyu Shi, and Jeffrey D. Hartgerink*

Departments of Chemistry and Bioengineering, Rice University, 6100 Main Street, Houston, Texas 77030, United States

Abstract

Controlling perioperative bleeding is of critical importance to minimize hemorrhaging and fatality. Patients on anticoagulant therapy such as heparin have diminished clotting potential and are at risk for hemorrhaging. Here we describe a self-assembling nanofibrous peptide hydrogel (termed SLac) that on its own can act as a physical barrier to blood loss. SLac was loaded with snake-venom derived Batroxobin (50 $\mu\text{g}/\text{mL}$) yielding a drug-loaded hydrogel (SB50). SB50 was potentiated to enhance clotting even in the presence of heparin. In vitro evaluation of fibrin and whole blood clotting helped identify appropriate concentrations for hemostasis in vivo. Batroxobin-loaded hydrogels rapidly (within 20s) stop bleeding in both normal and heparin-treated rats in a lateral liver incision model. Compared to standard of care, Gelfoam, and investigational hemostats such as Puramatrix, only SB50 showed rapid liver incision hemostasis post surgical application. This snake venom-loaded peptide hydrogel can be applied via syringe and conforms to the wound site resulting in hemostasis. This demonstrates a facile method for surgical hemostasis even in the presence of anticoagulant therapies.

Graphical abstract



*Corresponding Author: jdh@rice.edu. Tel: (713) 348-4142. Department of Chemistry, Department of Bioengineering, Rice University, Mail Stop 60, 6100 Main St., Houston, TX 77030, United States.

Supporting Information

The Supporting Information is available free of charge on the ACS Publications website at DOI: 10.1021/acsbomaterials.5b00356

Video demonstrating bleeding from the new incision compared to maintenance of hemostasis in the first SB50 clotted wound: double bleed experiment (AVI)

Author Contributions

The manuscript was written through contributions of all authors. All authors have given approval to the final version of the manuscript. The experiments were designed by V.A.K., S.S., and J.D.H., carried out by V.A.K., N.C.W., S.S. and interpreted by V.A.K., N.C.W., S.S., and J.D.H. The manuscript was written by V.A.K., N.C.W., S.S., and J.D.H.

The authors declare no competing financial interest.

Keywords

self-assembly; supramolecular chemistry; multidomain peptide; hemostasis

INTRODUCTION

Minimizing perioperative surgical bleeding is essential to ensuring optimal outcomes and limiting morbidity and mortality.¹⁻⁴ Excessive bleeding disrupts hemodynamics, requires transfusions, and prolongs operative time, burdening the healthcare system.^{4,5} The critical design requirement for hemostats are to (1) provide a localized conformal physical barrier to entrap red blood cells (RBC), (2) provide a chemical platform that accelerates clotting regardless of the presence of heparin, (3) stop bleeding in a rapid fashion (<1 min), and (4) prevent hemorrhaging during subsequent manipulation.⁶⁻⁹ Classic approaches for controlling intraoperative and perioperative bleeding involve use of physical pressure and sutures.^{2,6,10} Sutureless techniques typically involve foams, sealants, and adhesives; synthetic hemostats are typically made of cyanoacrylates, polyurethanes, and polyethylene glycol.^{2,9,11,12} These hemostats can result in toxic byproducts of polymerization/degradation, solvents, and immediate tissue necrosis in addition to local irritation and inflammation. Biologically derived adhesives are typically protein-based (collagen, fibrin, gelatin) or polysaccharide-based (starch, dextran). These materials suffer from batch-to-batch variability, are xeno-/allo-genic and therefore carry risk of latent biologic contamination.⁶ Commercially available GelFoam is a porcine derived lyophilized collagen substrate to physically absorb and block bleeding. In addition it has domains in the collagen which can modulate binding to vWF (von Willebrand Factor), platelets, macrophages, and subsequent activation of intrinsic and extrinsic coagulation pathways. Nevertheless, concerns with immunogenicity of the xenogenic collagen source, solid degradation products that may result in thromboemboli, and inhibition by anticoagulants have limited its utility. Design of materials that mimic the extracellular matrix, while providing unique clotting potential, is consequently an important biomaterials goal.^{2,8,11}

Thrombin potentiation of fibrin clot formation is inhibited with heparin and heparin based anticoagulants.^{13,14} Certain snake venom toxins have been known to aid in hemostasis.¹⁴⁻¹⁸ Batroxobin (Bax) is a snake venom-derived serine proteinase described nearly a century ago, 1936.¹⁹ Batroxobin present in venom is a potent heparin agnostic coagulant, able to cleave fibrinopeptide A at a nonheparin inhibited active site.^{18,20} Although a potent toxin found in snake venom to potentiate coagulation, batroxobin used clinically is recombinantly expressed in *E. coli* or *Pichia pastoris*, and purified to avoid toxicity concerns from contaminant snake venom.^{19,21-23} Use of batroxobin in medicine has been bolstered by a large body of work that has demonstrated safety and lack of systemic toxicity.^{19,22,23} Further, batroxobin is the active ingredient in FDA approved intravenous defibrinogenation (Defibrase) therapy; and is used at significantly higher concentrations than used for topical hemostasis in this study.^{19,21} Additionally, batroxobin is used in in vitro diagnostics to determine whole blood clotting time in the presence of heparin contamination (Reptilase Time, RT).²⁴⁻²⁸ However, batroxobin's use as a surgical hemostat is limited.^{19,21-23,29} Because it is a small, highly soluble molecule, localization at the wound site is not possible.

Multidomain peptides (MDP) have a distinct nanofibrillar morphology (2 nm thick, 6 nm wide, and nanometer to micrometer long) similar to extracellular matrix.^{30,31} Coupled with incorporation of fibronectin-derived sequences (-RGDS), cell friendly ECM mimics, MDP are capable of sustaining cell adhesion and proliferation.³² In this study, the MDP utilized has the sequence: KSLSLSLRGSLSLSLKGRGDS. This MDP, named “SLac”, has a cell adhesion sequence (-RGDS) as well as a MMP-2 cleavage site (-LRG).^{33–35} Loading of cytokines and growth factors via noncovalent physisorption onto matrix nanofibers has allowed for modulation of in vitro and in vivo responses.^{32,36} Subsequent to mechanical shear, storage modulus of shear thinning MDP shows near full recovery. Thus, nanofibers can be syringe loaded and delivered via needle or transcatheter.³⁷ These self-assembling nanofibers exhibit well controlled drug delivery and release characteristics.^{30,33–35} Additionally, base MDP sequences described in this study, MDP sequences modified with alternative bioactive sequences, and MDP loaded with drugs have shown excellent local and systemic biocompatibility, rapidly infiltrating with host cells, that secrete native matrix, and resolve over a 2–3 week period in vivo.^{30,31,33,35,38}

This study outlines the potential of a novel surgical hemostat based on batroxobin and MDP (combination termed SB50). All materials and hemostats used in this study are noted in Table 1. In vitro fibrin clot formation and whole blood clotting alone or in the presence of heparin helped determine appropriate dose concentrations. In vivo efficacy was demonstrated in a rat lateral liver incision model with subsequent surgical manipulation. The tests detailed herein help identify SB50 as an injectable surgical hemostat that (1) provides an injectable conformal physical barrier to the wound site, (2) provides a biochemical enzymatic platform that accelerates clotting agnostic of heparin, (3) clots blood within 20 s, and (4) keeps the wound site closed even after surgical manipulation.

EXPERIMENTAL SECTION

Peptide Synthesis and BAX Loading

Peptide Design and Characterization—Multidomain peptide SLac (K(SL)3(RG)(SL)-3KGRGDS) was prepared as previously published^{39,40} using standard solid phase peptide synthesis methods. Briefly, synthesis was performed on an Apex Focus XC (Aapptec) apparatus using Rink amide resin with 0.37 mM loading and N-terminal acetylation. Peptides were cleaved from resin, dialyzed, lyophilized and confirmed for purity using electrospray MALDI-TOF (Bruker Instruments, Billerica, MA). Peptide solutions were made by dissolving lyophilized SLac in 298 mM sucrose-water at a concentration of 2 w%, pH 7.4. Hydrogels were constructed by addition of Hank’s balanced salt solution (HBSS) at a 1:1 ratio. For gels containing batroxobin, batroxobin was dissolved in PBS and loaded into MDP hydrogel (100 μ L of SLac dissolved in 298 mM sucrose +100 μ L of 50ug/mL batroxobin in saline) in microcentrifuge tubes. Thus, final peptide concentration in hydrogels was 1 w%. Negatively charged polyvalent ions in buffer solution formed intermolecular ion interactions with lysine residues, cross-linking the hydrogel.

Rheology

Rheological behavior of peptide hydrogels was determined using 8 mm parallel plate geometry at a gap of 500 μm . 50 μL of hydrogel was placed on stainless steel plates of a rheometer (AR-G2, TA Instruments). A shear recovery experiment (1% strain for 30 min, 100% strain for 60 s, 1% strain for 30 min) was performed. Phase angle was maintained at 90° to ensure no slipping.

Fibrinogen Clotting

Hydrogel samples were cast in 96-well plates to cover the bottom of the well (50 μL ; $n = 4$). Fifty microliters of 4 mg/mL human fibrinogen in Tris-HCl (20 mM, pH 7.5) was added to each well. In a subset of experiments, Tris-HCl fibrinogen solution contained 0.9 IU/mL heparin, the clinical standard for blood heparin level. Clotting was monitored using real time measurements of clot turbidity at 405 nm taken every 30 s for 40–80 min.

Whole Blood Clotting

All studies were approved by the Rice Institutional Review Board. Three mL blood was collected in a plastic syringe. This initial draw was discarded to prevent tissue thromboplastin contamination. Blood collection was either in an acidified citrate dextrose (ACD) tube or a heparinized tube. 100 μL hydrogel samples ($n = 4$) were cast in each well of a 48-well plate. 500 μL of 0.1 M CaCl_2 was added to 5 mL of whole blood. One hundred microliters of blood was immediately added to samples. The 48-well plate was incubated at 37 °C. At 5 min, 1 mL of distilled water was added to each well to lyse red blood cells not trapped within the clot. Two hundred microliters of diluted hemoglobin released from lysed RBC was added to a 96-well plate and read for absorbance at 540 nm.

In Vivo Studies–Lateral Liver Incision Model

All experiments were approved by the Rice University Institutional Animal Care and Use committee. Female Wistar rats (225–250 g, Charles River Laboratories, Wilmington, MA) were used in this study, $n = 4$ animals for each material tested. Rats were anesthetized using isoflurane (2% for induction and 1% for maintenance). A vertical incision was made from xyphoid to the pubis, cutting through skin, fascia and muscle layers. A transverse cut was made in the left lobe of the exposed liver and site of bleeding treated with 100 μL of test material (SLac, Bax alone, SLac + Bax, GelFoam, Puramatrix (RADA-16) peptide gel 1% w/v) for hemostasis. Time taken for bleeding to stop was measured in each case. A subset of animals was pretreated 3 min prior to liver incision with heparin (400 IU/kg) through the IVC to determine hemostasis in the presence of an anticoagulant. Two minutes posthemostasis, the surgical wound was wiped with gauze and manually disrupted with forceps to determine bleeding potential.

RESULTS AND DISCUSSION

Synthesis and Rheological Properties

Of clinical importance is the chemical synthesis of these peptides. Because they are made via solid phase peptide synthesis, there is a significantly reduced concern of: (i) endotoxin

contamination from expression systems, (ii) xenogenic antigenicity, and (iii) batch-to-batch variability.^{41–48} Viscoelastic MDP are capable of shear thinning and rapid recovery. The storage modulus (G'), loss modulus (G''), and shear recovery of the SB50 gel (containing MDP SLac and 50 μ g/mL Batroxobin) is comparable to previously published MDP^{33–35,49,50} (Figure 1). Importantly, under intermittent high shear rates, peptide hydrogels recover to preshear G' values within 60 s. Together these results suggest the ability to use a material, which is easily injectable, and that can re-self-assemble to form a strong conformal gel, presenting a physical barrier to bleeding.^{6–8,51}

In Vitro Clotting

Analysis of hydrogels' suitability for hemostasis was verified using in vitro fibrin and whole blood clotting to screen formulations and concentrations. Fibrin network formation was initiated by addition of fibrinogen to samples. Turbidity measurements to compare fibrin clot formation showed a dependence on the presence of a hemostatic agent. Thrombin, positive control, showed the most rapid clotting time (Figure 2). Batroxobin addition demonstrated a dose dependent response. Loading of batroxobin into MDP created a hemostatic hydrogel that resulted in fibrin polymerization. Addition of heparin resulted in slower clotting times, especially for thrombin. Batroxobin addition resulted in rapid formation of fibrin clots even in the presence of heparin (Figure 2). Whole blood clotting times were measured similarly. Heparinized and nonheparinized human blood was clotted with a variety of materials. Clots that formed on material surfaces trapped RBC within fibrin matrices. Free RBC, outside of the clot, were lysed with excess DI water. Consequently, higher absorbance values indicate increased hemoglobin presence due to smaller clots entrapping fewer RBC on materials (Figure 3). Thrombin addition resulted in the most rapid clot formation. However, thrombin addition was ineffective in promoting hemostasis in the presence of heparin. Conversely, batroxobin showed the ability to clot heparinized blood.⁵² MDP hydrogels containing batroxobin (SB50) showed significantly greater clot formation in heparinized blood. From results demonstrating rapid hemostasis, SB50 was identified as the formulation of choice for in vivo studies.

In Vivo Clotting Potential

In vivo hemostasis efficacy was assessed using a lateral liver incision model. A 10–15 mm lateral incision was made on the left lobe of the liver in Wistar rats. The clotting potential of MDP (SLac), batroxobin (Bax50), standard-of-care (GelFoam), an alternative self-assembling hemostat Puramatrix (RADA-16),^{6,7} and SB50 was determined. In nonheparinized rats, SB50 demonstrated the most rapid hemostasis in 6s (Table 2). Batroxobin control showed minimal hemostasis as the aqueous solution rapidly flowed out of the incision site once applied; bleeding was not affected and hemostasis did not occur. After application of the hemostat, a 2 min waiting period was observed prior to tweezer manipulation of the incision. Both the control SLac gel and Bax50 resulted in a significant amount of bleeding upon site perturbation. SB50 group showed no bleeding even after extensive disruption of the site with tweezers (Figure 4). Heparinized rats showed a marked increase in time for hemostasis for all groups except SB50. Gelfoam application did not result in hemostasis within the experimental period. Puramatrix peptide gels demonstrated a bleeding time of (19 \pm 2 s) in heparinized rats, but continued to bleed after wound site

perturbation. (Table 2, Figure 5). SB50 proved effective in attenuating bleeding within 5 s, with hemostasis maintenance after wound perturbation. A subsequent incision in SB50 clotted wounds demonstrated bleeding from the new incision compared to maintenance of hemostasis in the first SB50 clotted wound: double bleed experiment (Video S1). In the double bleed model, hemostasis was preserved after surgical manipulation when treated with SB50, with demonstration of a secondary rapid bleed site.

CONCLUSION

Batroxobin released from MDP hydrogels clots blood while conforming to the surgical defect. Fibrinogen and whole blood clotting assays both showed the bioavailability and functionality of batroxobin and batroxobin released from MDP hydrogel. The clotting ability of batroxobin was not inhibited by heparin, as it is by thrombin. SB50 showed rapid hemostasis even after wound site manipulation, compared to other standard of care or peptide-based hemostat controls. Together this may present a novel tool in the arsenal for surgical hemostasis in patients on anticoagulant therapy.

Supplementary Material

Refer to Web version on PubMed Central for supplementary material.

Acknowledgments

Funding: The work presented in this manuscript was support by grants from the National Institute of Health for J.D.H. (R01 DE021798) and V.A.K. (F32 DE023696). Additional support was provided by the Welch Foundation grant C-1557

References

1. Scognamiglio F, Travan A, Rustighi I, Tarchi P, Palmisano S, Marsich E, Borgogna M, Donati I, de Manzini N, Paoletti S. Adhesive and Sealant Interfaces for General Surgery Applications. *J Biomed Mater Res, Part B*. 2015;10:33409.
2. Ghobril C, Grinstaff MW. The Chemistry Engineering of Polymeric Hydrogel Adhesives for Wound Closure: A Tutorial. *Chem Soc Rev*. 2015; 44:1820–1835. [PubMed: 25649260]
3. Cheng CM, Meyer-Massetti C, Kayser SRA. Review of Three Stand-Alone Topical Thrombins for Surgical Hemostasis. *Clin Ther*. 2009; 31:32–41. [PubMed: 19243705]
4. Martyn D, Kocharian R, Lim S, Meckley LM, Miyasato G, Prifti K, Rao Y, Rieberman JB, Scaife JG, Soneji Y, Corral M. Reduction in Hospital Costs Resource Consumption Associated with the Use of Advanced Topical Hemostats During Inpatient Procedures. *J Med Econ*. 2015; 18:474–481. [PubMed: 25728820]
5. Mehdizadeh M, Yang J. Design Strategies Applications of Tissue Bioadhesives. *Macromol Biosci*. 2013; 13:271–288. [PubMed: 23225776]
6. Csukas D, Urbanics R, Moritz A, Ellis-Behnke R. Ac5 Surgical Hemostat as an Effective Hemostatic Agent in an Anti-coagulated Rat Liver Punch Biopsy Model. *Nanomedicine*. 2015; 11:2025. [PubMed: 25597908]
7. Ellis-Behnke RG, Liang YX, Tay DK, Kau PW, Schneider GE, Zhang S, Wu W, So KF. Nano Hemostat Solution: Immediate Hemostasis at the Nanoscale. *Nanomedicine*. 2006; 2:207–215. [PubMed: 17292144]
8. Kumar VA, Taylor NL, Jalan AA, Hwang LK, Wang BK, Hartgerink JD. A Nanostructured Synthetic Collagen Mimic for Hemostasis. *Biomacromolecules*. 2014; 15:1484–1490. [PubMed: 24694012]

9. Gabay M, Boucher BA. An Essential Primer for Understanding the Role of Topical Hemostats Surgical Sealants Adhesives for Maintaining Hemostasis. *Pharmacotherapy*. 2013; 33:935–955. [PubMed: 23686938]
10. Chan LW, White NJ, Pun SH. Synthetic Strategies for Engineering Intravenous Hemostats. *Bioconjugate Chem*. 2015; 26:1224–1236.
11. Sanders L, Nagatomi J. Clinical Applications of Surgical Adhesives Sealants. *Crit Rev Biomed Eng*. 2014; 42:271–292. [PubMed: 25597240]
12. Broekema FI, van Oeveren W, Selten MH, Meijer RJ, de Wolf JT, Bos RR. In Vivo Hemostatic Efficacy of Polyurethane Foam Compared to Collagen Gelatin. *Clin Oral Investig*. 2013; 17:1273–1278.
13. Smith SA, Travers RJ, Morrissey JH. How It All Starts: Initiation of the Clotting Cascade. *Crit Rev Biochem Mol Biol*. 2015; 50:326–336. [PubMed: 26018600]
14. Blomback B. Fibrin Formation in Whole Blood. *Thromb Res*. 2000; 99:307–310. [PubMed: 11203134]
15. Petretski JH, Kanashiro M, Silva CP, Alves EW, Kipnis TL. Two Related Thrombin-Like Enzymes Present in Bothrops Atriox Venom. *Braz J Med Biol Res*. 2000; 33:1293–1300. [PubMed: 11050658]
16. Urano T, Ihara H, Takada Y, Fujie M, Takada A. The Cleavage Inactivation of Plasminogen Activator Inhibitor Type 1 Alpha2-Antiplasmin by Reptilase a Thrombin-Like Venom Enzyme. *Blood Coagulation Fibrinolysis*. 2000; 11:145–153. [PubMed: 10759007]
17. Maruyama M, Kamiguti AS, Cardoso JL, Sano-Martins IS, Chudzinski AM, Santoro ML, Morena P, Tomy SC, Antonio LC, Mihara H, et al. Studies on Blood Coagulation and Fibrinolysis in Patients Bitten by Bothrops Jararaca (Jararaca). *Thromb Haemost*. 1990; 63:449–453. [PubMed: 2402749]
18. Klocking HP, Markwardt F, Guttner J. On the Mechanism of Batroxobin-Induced Fibrinolysis. *Pharmazie*. 1989; 44:504–505. [PubMed: 2510188]
19. Serrano SM. The Long Road of Research on Snake Venom Serine Proteinases. *Toxicon*. 2013; 62:19–26. [PubMed: 23010164]
20. Weisel JW. Which Knobs Fit into Which Holes in Fibrin Polymerization? *J Thromb Haemostasis*. 2007; 5:2340–2343. [PubMed: 17922803]
21. Braud S, Bon C, Wisner A. Snake Venom Proteins Acting on Hemostasis. *Biochimie*. 2000; 82:851–859. [PubMed: 11086215]
22. Yamazaki Y, Morita T. Snake Venom Components Affecting Blood Coagulation the Vascular System: Structural Similarities Marked Diversity. *Curr Pharm Des*. 2007; 13:2872–2886. [PubMed: 17979732]
23. Lu Q, Clemetson JM, Clemetson KJ. Snake Venoms Hemostasis. *J Thromb Haemostasis*. 2005; 3:1791–1799. [PubMed: 16102046]
24. Bell WR Jr. Defibrinogenating Enzymes. *Drugs*. 1997; 54(Suppl 3):18–30. [PubMed: 9360849]
25. Castro HC, Zingali RB, Albuquerque MG, Pujol-Luz M, Rodrigues CR. Snake Venom Thrombin-Like Enzymes: From Reptilase to Now. *Cell Mol Life Sci*. 2004; 61:843–856. [PubMed: 15095007]
26. Yang Y, Tian SJ, Wu L, Huang DH, Wu WP. Fibrinogen Depleting Agent Batroxobin Has a Beneficial Effect on Experimental Autoimmune Encephalomyelitis. *Cell Mol Neurobiol*. 2011; 31:437–448. [PubMed: 21165693]
27. Hao Z, Liu M, Counsell C, Wardlaw JM, Lin S, Zhao X. Fibrinogen Depleting Agents for Acute Ischaemic Stroke. *Cochrane Database Syst Rev*. 2012; 3:CD000091. [PubMed: 22419274]
28. Karapetian H. Reptilase Time (Rt). *Methods Mol Biol*. 2013; 992:273–277. [PubMed: 23546720]
29. You KE, Koo MA, Lee DH, Kwon BJ, Lee MH, Hyon SH, Seomun Y, Kim JT, Park JC. The Effective Control of a Bleeding Injury Using a Medical Adhesive Containing Batroxobin. *Biomed Mater*. 2014; 9:025002. [PubMed: 24487019]
30. Kumar VA, Taylor NL, Shi S, Wang BK, Jalan AA, Kang MK, Wickremasinghe NC, Hartgerink JD. Highly Angiogenic Peptide Nanofibers. *ACS Nano*. 2015; 9:860–868. [PubMed: 25584521]

31. Wickremasinghe NC, Kumar VA, Hartgerink JD. Two-Step Self-Assembly of Liposome-Multidomain Peptide Nanofiber Hydrogel for Time-Controlled Release. *Biomacromolecules*. 2014; 15:3587–3595. [PubMed: 25308335]
32. Galler KM, D'Souza RN, Federlin M, Cavender AC, Hartgerink JD, Hecker S, Schmalz G. Dentin Conditioning Codetermines Cell Fate in Regenerative Endodontics. *J Endod*. 2011; 37:1536–1541. [PubMed: 22000458]
33. Kumar VA, Shi S, Wang BK, Li IC, Jalan AA, Sarkar B, Wickremasinghe NC, Hartgerink JD. Drug-Triggered Cross-Linked Self-Assembling Nanofibrous Hydrogels. *J Am Chem Soc*. 2015; 137:4823–4830. [PubMed: 25831137]
34. Kumar VA, Taylor NL, Shi S, Wang BK, Jalan AA, Kang MK, Wickremasinghe NC, Hartgerink JD. Highly Angiogenic Peptide Nanofibers. *ACS Nano*. 2015; 9:860–868. [PubMed: 25584521]
35. Kumar VA, Taylor NL, Shi S, Wickremasinghe NC, D'Souza RN, Hartgerink JD. Self-Assembling Multidomain Peptides Tailor Biological Responses through Biphasic Release. *Biomaterials*. 2015; 52:71–78. [PubMed: 25818414]
36. Galler KM, Hartgerink JD, Cavender AC, Schmalz G, D'Souza RN. A Customized Self-Assembling Peptide Hydrogel for Dental Pulp Tissue Engineering. *Tissue Eng, Part A*. 2012; 18:176–184. [PubMed: 21827280]
37. Wang Y, Bakota E, Chang BH, Entman M, Hartgerink JD, Danesh FR. Peptide Nanofibers Preconditioned with Stem Cell Secretome Are Renoprotective. *J Am Soc Nephrol*. 2011; 22:704–717. [PubMed: 21415151]
38. Wickremasinghe NC, Kumar VA, Shi S, Hartgerink JD. Controlled Angiogenesis in Peptide Nanofiber Composite Hydrogels. *ACS Biomater Sci Eng*. 2015; 1:845–854.
39. Dong H, Paramonov SE, Aulisa L, Bakota EL, Hartgerink JD. Self-Assembly of Multidomain Peptides: Balancing Molecular Frustration Controls Conformation Nanostructure. *J Am Chem Soc*. 2007; 129:12468–12472. [PubMed: 17894489]
40. Aulisa L, Dong H, Hartgerink JD. Self-Assembly of Multidomain Peptides: Sequence Variation Allows Control over Cross-Linking Viscoelasticity. *Biomacromolecules*. 2009; 10:2694–2698. [PubMed: 19705838]
41. Liu L, Liu X, Deng H, Wu Z, Zhang J, Cen B, Xu Q, Ji A. Something between the Amazing Functions Various Morphologies of Self-Assembling Peptides Materials in the Medical Field. *J Biomater Sci Polym Ed*. 2014; 25:1331–1345. [PubMed: 25088690]
42. Nagarkar RP, Schneider JP. Synthesis Primary Characterization of Self-Assembled Peptide-Based Hydrogels. *Methods Mol Biol*. 2008; 474:61–77. [PubMed: 19031061]
43. Vemula PK, Wiradharma N, Ankrum JA, Miranda OR, John G, Karp JM. Prodrugs as Self-Assembled Hydrogels: A New Paradigm for Biomaterials. *Curr Opin Biotechnol*. 2013; 24:1174–1182. [PubMed: 23465753]
44. Zhang S. Molecular Self-Assembly: Another Brick in the Wall. *Nat Nanotechnol*. 2006; 1:169–170. [PubMed: 18654179]
45. Hudalla GA, Sun T, Gasiorowski JZ, Han H, Tian YF, Chong AS, Collier JH. Graded Assembly of Multiple Proteins into Supramolecular Nanomaterials. *Nat Mater*. 2014; 13:829–836. [PubMed: 24930032]
46. Mora-Solano C, Collier JH. Engaging Adaptive Immunity with Biomaterials. *J Mater Chem B*. 2014; 2:2409–2421.
47. Jung JP, Gasiorowski JZ, Collier JH. Fibrillar Peptide Gels in Biotechnology Biomedicine. *Biopolymers*. 2010; 94:49–59. [PubMed: 20091870]
48. Rudra JS, Tian YF, Jung JP, Collier JH. A Self-Assembling Peptide Acting as an Immune Adjuvant. *Proc Natl Acad Sci USA*. 2010; 107:622–627. [PubMed: 20080728]
49. Galler KM, Aulisa L, Regan KR, D'Souza RN, Hartgerink JD. Self-Assembling Multidomain Peptide Hydrogels: Designed Susceptibility to Enzymatic Cleavage Allows Enhanced Cell Migration Spreading. *J Am Chem Soc*. 2010; 132:3217–3223. [PubMed: 20158218]
50. Galler KM, Hartgerink JD, Cavender AC, Schmalz G, D'Souza RN. A Customized Self-Assembling Peptide Hydrogel for Dental Pulp Tissue Engineering. *Tissue Eng Part A*. 2012; 18:176–184. [PubMed: 21827280]

51. Komatsu S, Nagai Y, Naruse K, Kimata Y. The Neutral Self-Assembling Peptide Hydrogel Spg-178 as a Topical Hemostatic Agent. *PLoS One*. 2014; 9:e102778. [PubMed: 25047639]
52. Vu TT, Stafford AR, Leslie BA, Kim PY, Fredenburgh JC, Weitz JI. Batroxobin Binds Fibrin with Higher Affinity Promotes Clot Expansion to a Greater Extent Than Thrombin. *J Biol Chem*. 2013; 288:16862–16871. [PubMed: 23612970]

Author Manuscript

Author Manuscript

Author Manuscript

Author Manuscript

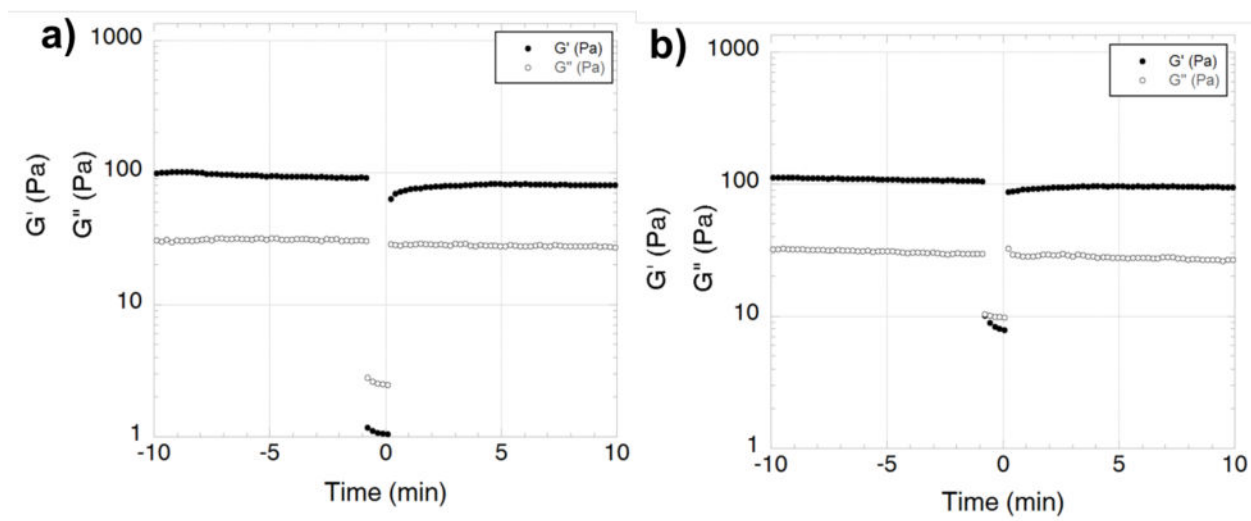


Figure 1.

Shear recovery of (a) SLac gel and (b) SB50 gel. Addition of Batroxobin has not altered the typical rheological properties of the hydrogel. SB50 demonstrates ability to recover from shear stress. Shear recovery was performed at 1% strain for 30 min, 100% strain for 60 s, and returned to 1% strain for 30 min. During high strain (100%) G' and G'' values invert indicating liquefaction of hydrogels under high shear, with G' value returning within a minute after return of low strain rate.

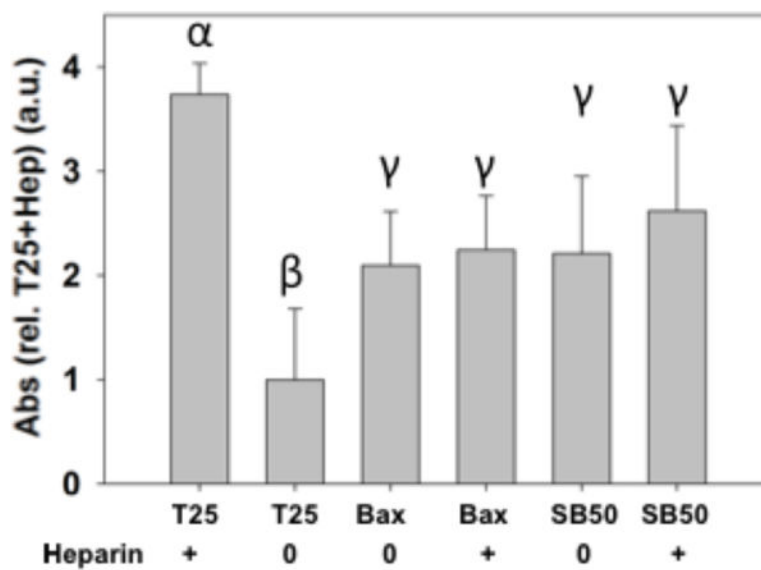


Figure 2. Fibrinogen clot formation. Batroxobin addition resulted in more rapid clotting even in the presence of heparin (0.9 IU/mL heparin). Thrombin activity was shown to be inhibited in the presence of heparin. SB50 showed similar clotting potential to Bax regardless of heparin presence. Similar Greek letter indicates no statistically significant difference ($*p < 0.05$).

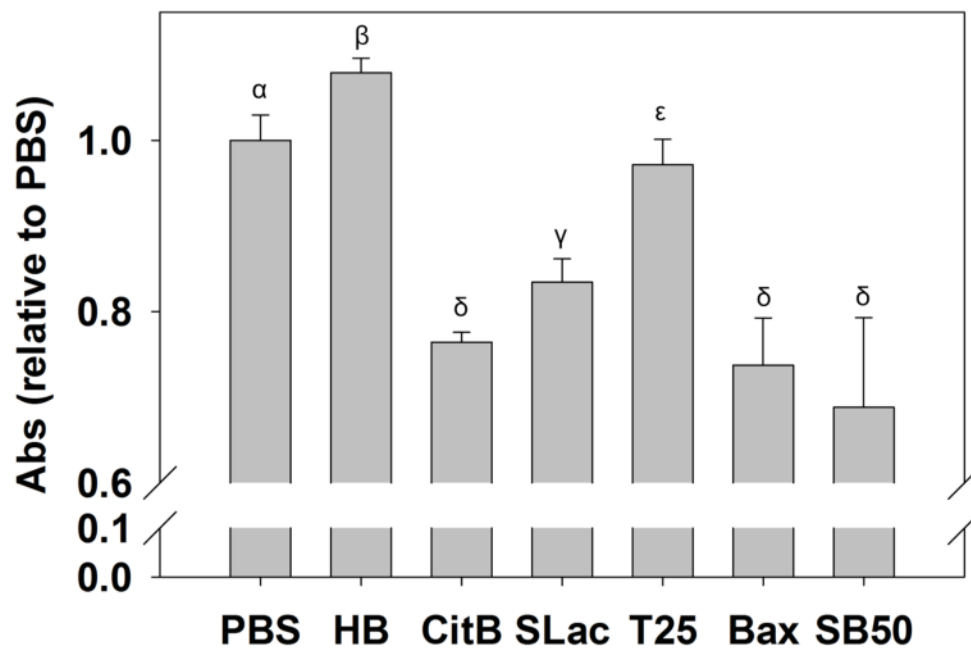


Figure 3. Whole blood clotting. Scaffolds were incubated with heparinized whole blood. Free RBC, outside of the clot, were lysed and absorbance measured. SB50 showed the rapid clotting (lowest free RBC absorbance). Data normalized to PBS: phosphate buffered saline addition, negative control. HB: heparinized blood showed slowest clotting time. CitB: citrate clotted with Ca^{2+} , positive control. Nomenclature for all samples in Table 1. Similar Greek letter indicates no statistically significant difference ($*p < 0.05$).

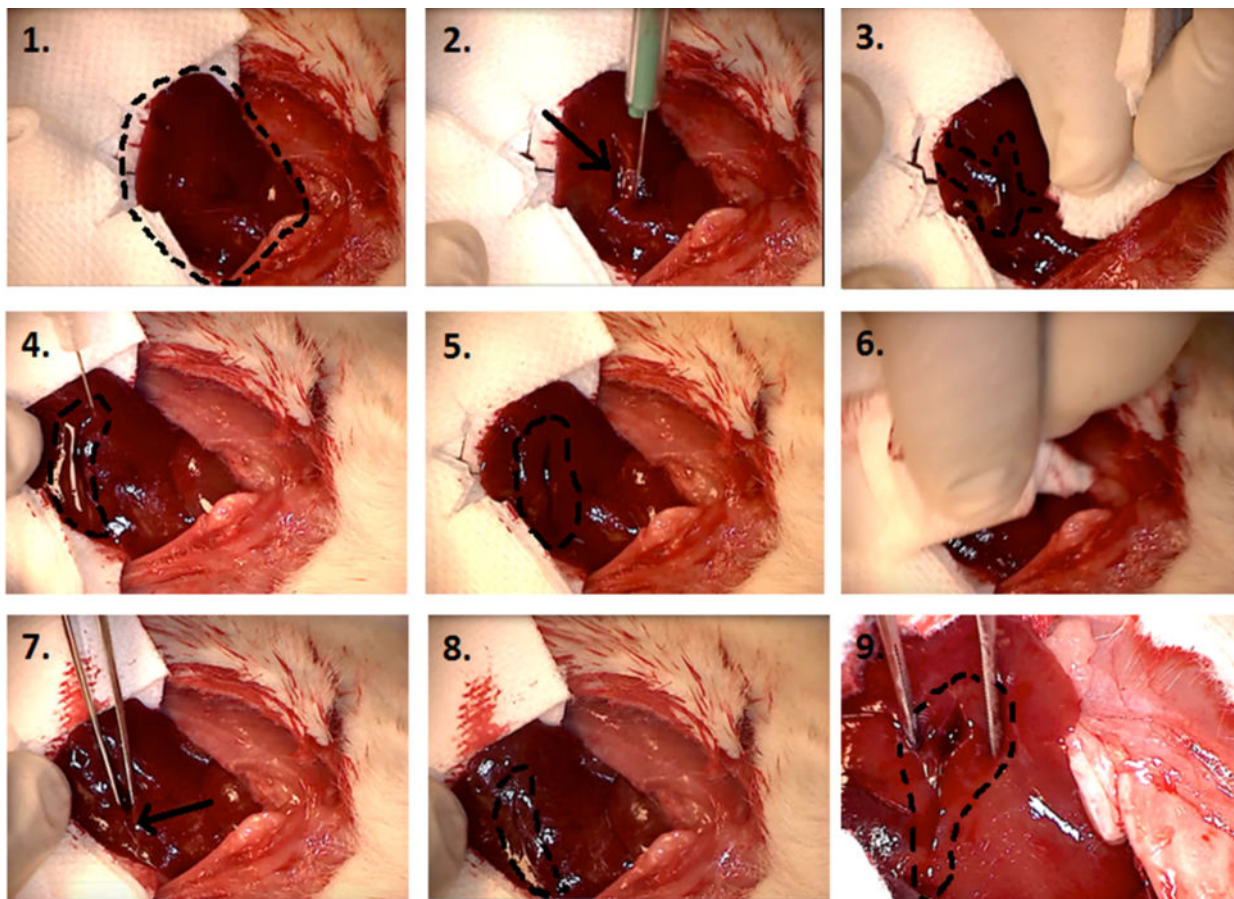


Figure 4.

Liver incision model: step-by-step procedure in applying SB50. 1. Exposed left lobe of liver preincision (right cranial, left caudal). 2. Immediately after lateral incision by scalpel (arrow points at incision). 3. Profuse bleeding prior to application of SB50 gel (indicated by area marked by dotted line). 4. Application of SB50 gel after wiping cut with sterile gauze. Gel is localized to the area within the dotted line on image, right above the incision. 5. SB50 gel left on cut for 2 min. 6. SB50 gel is wiped away at the end of a 2 min waiting period. 7. Cut (indicated by arrow) is perturbed by probing with sterile tweezers. 8. No bleeding is observed even after excessive perturbation. Incision site is marked by dotted line. 9. Zoomed in image of cut showing no bleeding during site perturbation.

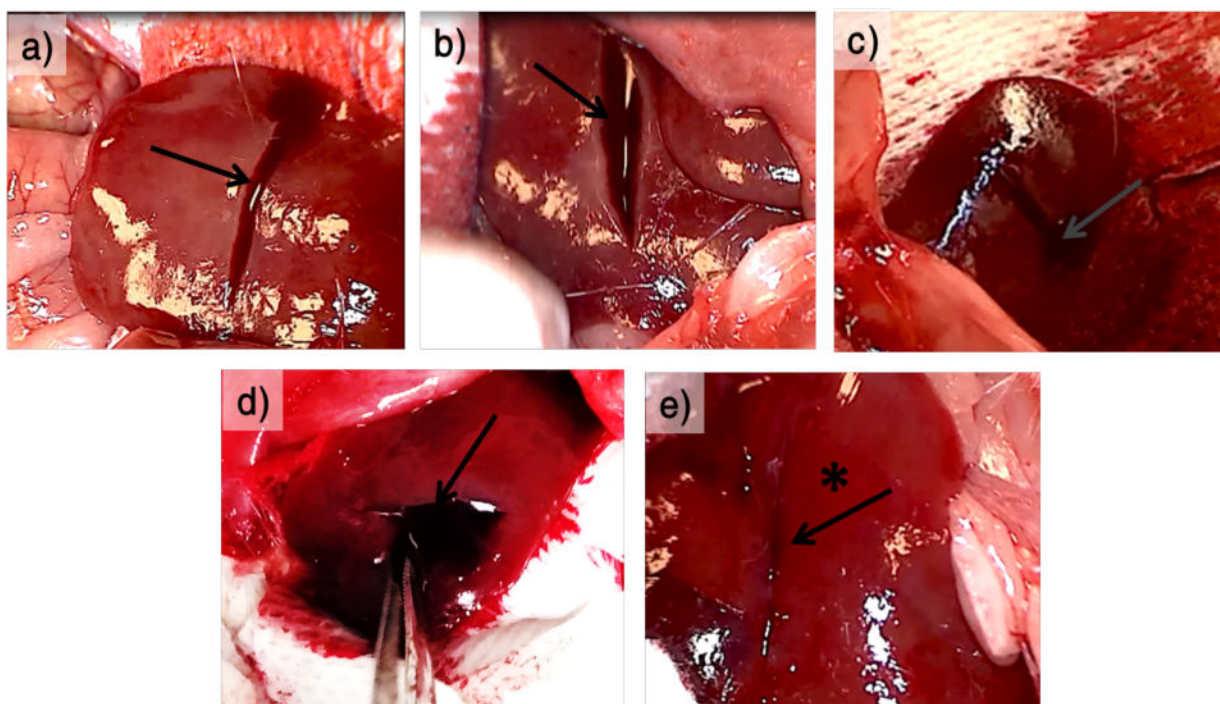


Figure 5. Liver incision in heparinized mice. The images show incision site in heparinized mice, post application of test material on incised left lobe of liver (right cranial, left caudal). (a) SLac gel, (b) Bax50, (c) GelFoam strip, (d) Puramatrix (RADA) gel, (e) SB50 gel. In each case, the test material is applied to incision site after wiping it with sterile gauze. It is kept for a waiting period of 2 min and wiped away. Profuse bleeding can be seen in every case (indicated by the arrows in a–d) except for when SB50 gel is applied (indicated by the asterisk and arrow in e)).

Table 1

Nomenclature and Composition of Hemostatic Materials Used in This Study

material	concentration		hemostat	mechanism of clotting
	peptide (wt %)	batroxobin ($\mu\text{g/mL}$)		
SB5	1	5	batroxobin	physical and biochemical hemostat
SB50	1	50	batroxobin	physical and biochemical hemostat
SLac	1	0	N/A	physical barrier
Bax	0	5	batroxobin	cleaves fibrin peptide A
Bax50	0	50	batroxobin	cleaves fibrin peptide A
T1	0	0	thrombin (25 $\mu\text{g/mL}$)	intrinsic pathway/extrinsic pathway

Author Manuscript

Author Manuscript

Author Manuscript

Author Manuscript

Table 2

In Vivo Hemostasis Response to SLac, Bax50, Gelfoam, and SB50^a

	no heparin			heparinized				
	SLac	Bax50	SB50	SLac	Bax50	SB50	Gelfoam ^b	Puramatrix ^b
time to hemostasis	11 s (± 2 s)	no hemo-stasis	6 s (± 1 s)	120 s (± 5 s)	no hemo-stasis	5 s (± 1 s)	no hemo-stasis	19 s (± 2 s)
initial bleeding ^c	++	++++	+	+++	++++	++	++	++
postbleeding ^c	+	++	none	++++	++++	+	++++	++++
perturbed bleeding ^c	+++	+++	none	++++	++++	none	++++	++++

^aNotation: + indicates degree of bleeding with + marginal bleeding absorbable with gauze, +++ moderate bleeding, and +++++ profuse bleeding.

^bGelfoam and Puramatrix (RADAI6) are commercially available materials that are known to form a physical barrier for hemostasis.

^cInitial bleeding: bleeding measured during the 2 min period immediately after application of hemostat. Postbleeding: bleeding after manual wiping of excess hemostat from the wound site using sterile gauze. Perturbed bleeding: Bleeding of the wound site after manipulation with forceps.